

Absorption-reduced waveguide structure for efficient terahertz generation

L. Pálfalvi,^{1,a)} J. A. Fülöp,^{2,3} and J. Hebling^{1,2,3}

¹*Institute of Physics, University of Pécs, Ifjúság ú. 6, 7624 Pécs, Hungary*

²*MTA-PTE High-Field Terahertz Research Group, Ifjúság ú. 6, 7624 Pécs, Hungary*

³*Szentágotthai Research Centre, University of Pécs, Ifjúság ú. 20, 7624 Pécs, Hungary*

(Received 15 August 2015; accepted 20 November 2015; published online 9 December 2015)

An absorption-reduced planar waveguide structure is proposed for increasing the efficiency of terahertz (THz) pulse generation by optical rectification of femtosecond laser pulses with tilted-pulse-front in highly nonlinear materials with large absorption coefficient. The structure functions as waveguide both for the optical pump and the generated THz radiation. Most of the THz power propagates inside the cladding with low THz absorption, thereby reducing losses and leading to the enhancement of the THz generation efficiency by up to more than one order of magnitude, as compared with a bulk medium. Such a source can be suitable for highly efficient THz pulse generation pumped by low-energy (nJ- μ J) pulses at high (MHz) repetition rates delivered by compact fiber lasers. © 2015 AIP Publishing LLC. [<http://dx.doi.org/10.1063/1.4937347>]

The recent years witnessed a rapid development of pulsed terahertz (THz) sources driven by femtosecond lasers, which became an enabling tool for new research directions such as nonlinear THz spectroscopy. THz sources with high peak intensity typically require pump pulses with mJ-level energy, thereby usually limiting the pulse repetition rate to the kHz range. Linear and nonlinear THz spectroscopic studies and other applications highly benefit from increased repetition rate, and there is a strong need to develop efficient THz sources with significantly higher (1–100 MHz) repetition rates. Fiber laser technology provides commercially available sources with superior stability and compactness delivering femtosecond pulses at high repetition rates but with moderate pulse energy (up to the 10- μ J level). It is challenging to design efficient THz sources based on optical rectification (OR) at these small or moderate pump pulse energies.

The efficiency of OR can be increased by cylindrical focusing, or by using waveguide or waveguide-like structures.^{1–9} In case of materials with high nonlinearity but strong absorption in the THz range, such as LiNbO₃ (LN) with $d_{33} = 168$ pm/V nonlinear optical coefficient¹⁰ and tens of cm⁻¹ absorption coefficient,¹¹ it is important to suppress absorption. A promising way to achieve this is to sandwich a few μ m thick LN layer between layers of significantly smaller absorption.^{1–5} A suitable material for such a low-absorption cladding is silicon (Si). The structures reported so far are guiding only the optical pump;^{1–5} the selected material parameters and dimensions do not allow wave guiding in the THz range. Consequently, the THz radiation leaves the LN layer through its boundary to the cladding. This reduces the propagation length of the generated THz radiation inside LN, thereby minimizing absorption losses. However, because of the reduced interaction length, the efficiency of THz generation is lower than it could be for a (velocity-matched) structure guiding both pump and THz. In the former case it is the intensity, while in the latter case it is the

field strength of the THz components generated at different locations, which is summed up. Latter can enable to achieve a significantly higher THz generation efficiency. Although such double-waveguide structures were already introduced for phase matching of THz generation by parametric interaction⁶ or optical rectification,⁸ the problem of absorption was nowhere mentioned in these works.

In this work, an absorption-reduced waveguide (ARWG) THz source is introduced where both the optical pump as well as the generated THz radiation are guided such that velocity matching is fulfilled for OR. The key point for efficient THz generation is that the THz waveguide has to have a cladding with orders of magnitude smaller absorption coefficient in the THz range than that of the core. Appropriate waveguide design ensures that 80%–95% of the THz energy propagates in the cladding. The absorption losses decrease with increasing fraction of power propagating in the cladding. Velocity matching is achieved by using the tilted-pulse-front pumping (TPFP) technique.¹²

The proposed absorption-reduced planar waveguide THz source consists of a common core for both the optical pump and the THz radiation (Fig. 1(a)), forming also the nonlinear medium for OR. We assume 0.67 mol. % MgO-doped stoichiometric LN as the core material, but other materials are also possible (e.g., ZnTe, GaP, CdTe, and DAST), where the absorption may originate from the usual

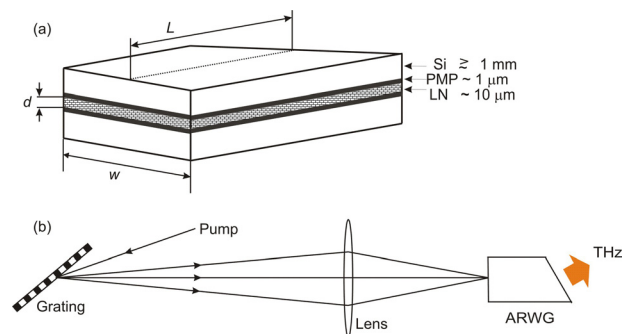


FIG. 1. (a) The ARWG structure. (b) The ARWG THz source with TFPF (top view).

^{a)}Author to whom correspondence should be addressed. Electronic mail: palfalvi@fizika.ttk.pte.hu

TABLE I. Optical refractive (n_p), optical group ($n_{g,p}$), and THz refractive (n_{THz}) indices, and the THz absorption coefficients (α_{THz}) for the materials used in the ARWG.

	n_p (1 μm)	$n_{g,p}$ (1 μm)	n_{THz} (1 THz)	α_{THz} (1 THz)
LN	2.15 (Ref. 14)	2.21 (Ref. 14)	4.96 (Ref. 11)	27.3 cm^{-1} (Ref. 11)
PMP	1.47 (Ref. 15)	not relevant	1.46 (Ref. 15)	$\sim 1.1 \text{ cm}^{-1}$ (Ref. 15)
Si	~ 3.5 (Ref. 5)	not relevant	3.42 (Ref. 16)	$\sim 0.05 \text{ cm}^{-1}$ (Ref. 16)

complex dielectric function or from free-carrier absorption generated by multiphoton absorption of the pump. LN has extremely large nonlinearity, but also significant absorption in the THz range (Table I), which reduces the pump-to-THz conversion efficiency.¹³ A suitable cladding material for guiding THz radiation generated in the LN core is silicon (Si). The absorption coefficient of Si is more than two orders of magnitude smaller than that of LN (Table I). The THz refractive indices of both LN and Si are larger than the group index of LN at the typical pump wavelength of 1 μm (Table I). In this situation, velocity matching can be achieved by TFPF in the plane of the LN core (Fig. 1(b)). Owing to the mode structure of the THz field in the Si-LN-Si waveguide (see also Fig. 3 inset), in practical situations (see below) it is enough if the thickness of the Si cladding is about 1 mm or larger.

As mentioned earlier, the ARWG THz source has to guide both the optical pump and the THz waves. However, for typical pump wavelengths, the refractive index of the Si cladding is larger than that of the LN core (Table I), which prohibits wave guiding in the optical range. To solve this problem (similarly to Ref. 5) an inner cladding was introduced between the LN core and the Si outer cladding (Fig. 1(a)). Suitable materials for the inner cladding are, for example, polymers having smaller optical refractive index than that of the LN core and low THz absorption.^{15,17} It should also be transparent in the optical wavelength range of interest. One suitable material is polymethylpentene (PMP, often referred to as TPX), frequently used for THz applications (Table I). The thickness of the PMP inner cladding is advantageously chosen in the same order of magnitude as the pump wavelength. By this choice the influence of the PMP layer on the THz wave is negligible. At the same time it also prohibits the penetration of the optical pump into the Si outer cladding, since its penetration depth into the PMP is by one order of magnitude smaller than the PMP thickness. This is important in order to avoid free-carrier generation in Si, which could induce absorption in the THz range. Besides creating the necessary pulse front tilt for velocity matching, the TFPF setup has to provide mode

matching of the incoming pump beam to the lowest-order mode of the inner PMP-LN-PMP waveguide. This can be easily achieved by inserting suitable (cylindrical) lenses either in front of or behind the grating.

Numerical simulations were carried out to explore the performance of the ARWG THz source. In the calculations, the influence of the PMP inner cladding on the THz wave was neglected due to its small absorption coefficient and small thickness. As mentioned earlier, the thickness of Si layer should be at least 1 mm in practice, which allows to neglect THz waveguide effects of the Si-air outer boundary. Hence, for the sake of simplicity, in the simulations a Si-LN-Si waveguide with an LN core of thickness d and a Si cladding of infinitely large thickness was considered. Waveguide dispersion for the pump was neglected. A pump wavelength of 1030 nm was assumed, which is typical for Yb-doped (fiber) lasers.

By applying Eqs. (7.2)–(20) of Ref. 18 for the lowest-order TE mode, one can obtain for the core thickness the following expression:

$$d = \frac{c}{\pi \nu n_{\text{eff,THz}} \sqrt{\left(\frac{n_1}{n_{\text{eff,THz}}}\right)^2 - 1}} \tan^{-1} \sqrt{\frac{1 - \left(\frac{n_2}{n_{\text{eff,THz}}}\right)^2}{\left(\frac{n_1}{n_{\text{eff,THz}}}\right)^2 - 1}}. \quad (1)$$

Here, c is the speed of light in vacuum, n_1 and n_2 are the refractive indices at the THz frequency ν of core and cladding, respectively, and $n_{\text{eff,THz}}$ is the desired effective refractive index with $n_{\text{Si,THz}} < n_{\text{eff,THz}} < n_{\text{LN,THz}}$. The necessary core thickness was plotted versus $n_{\text{eff,THz}}$ at a few selected frequencies between 0.5 THz and 2.5 THz in Fig. 2(a), and versus the THz frequency keeping the effective THz index of refraction at the constant value of $n_{\text{eff,THz}} = 3.8$ in Fig. 2(b).

Fig. 3 shows the power confinement ratio $P_{\text{core}}/P_{\text{total}}$ of the THz power accommodated inside the LN core and the total THz power, calculated from the transversal intensity distribution (see Chap. 7.2 of Ref. 18) of the lowest-order waveguide mode as a function of $n_{\text{eff,THz}}$. $P_{\text{core}}/P_{\text{total}}$ varies between 2% and 26% in the $n_{\text{eff,THz}} = 3.5$ to 4.0 range, independently from the THz frequency. These power ratio values are sufficiently low to support efficient THz generation even in highly absorbing core materials such as LN. It is also obvious from Fig. 3 that smaller $n_{\text{eff,THz}}$ values are more advantageous for reducing the effect of THz absorption.

The pulse front tilt angle γ needed for velocity matching of pump and THz can be determined from the equation

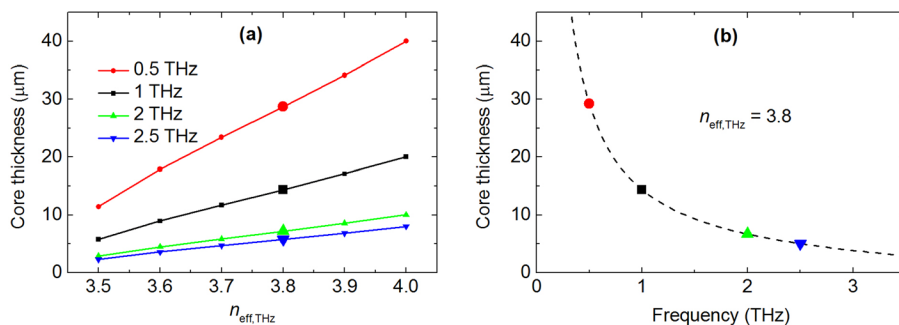


FIG. 2. Required core thickness of the Si-LN-Si THz waveguide versus the aimed effective THz refractive index for different THz frequencies (a) and versus the THz frequency for $n_{\text{eff,THz}} = 3.8$ (b). The large symbols of Figure 2(a) correspond to those in Figure 2(b).

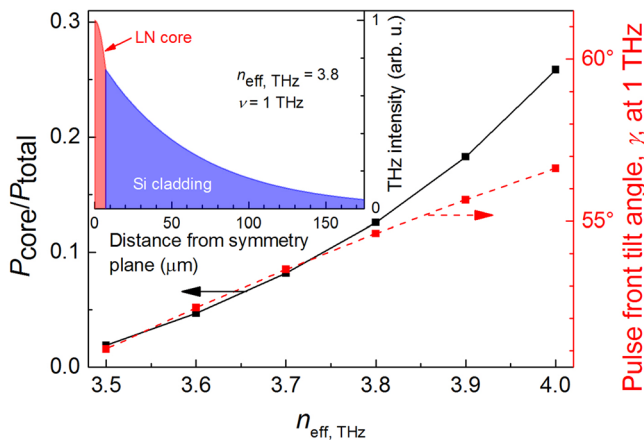


FIG. 3. The power confinement ratio $P_{\text{core}}/P_{\text{total}}$ (black solid line) and the pulse front tilt angle for 1 THz (red dashed line) versus the effective THz refractive index. The inset shows the THz intensity distribution for $n_{\text{eff, THz}} = 3.8$ versus the distance measured from the symmetry plane of the structure for 1 THz.

$c/n_{\text{eff, THz}} = (c/n_{\text{g, pump}}) \cos \gamma$.¹² The dependence of γ on $n_{\text{eff, THz}}$, assuming 1 THz frequency, is also shown in Fig. 3. Its value varies between 51° and 57° and is smaller than $\sim 63^\circ$, the value in bulk LN. This is advantageous for increasing the efficiency of the THz source, since a smaller pulse front tilt angle results in larger pump dispersion length and, consequently, in larger effective interaction length for THz generation.¹³ Besides the reduced absorption, this also contributes to the larger THz generation efficiency, as illustrated in Fig. 4 for OR of 10-nJ, 100-fs pulses (more details of the calculation are given later; see also Table II). Fig. 4(a) shows the variation of the pump pulse duration and Fig. 4(b) the build-up of the THz field, in terms of efficiency, along the propagation distance. The maximum efficiency is almost 20 times larger for the ARWG than for bulk LN. The effective interaction length can be defined as the distance needed to reach the maximum efficiency from 5%.¹³ A smaller $n_{\text{eff, THz}}$ value is more advantageous also in this respect, as it gives a smaller γ .

Table II summarizes possible ARWG design parameters for various typical laser parameters, together with the basic characteristics of the predicted THz output. To estimate the THz output, a similar model was used as in Ref. 19. The variation of the pump pulse duration during propagation owing to

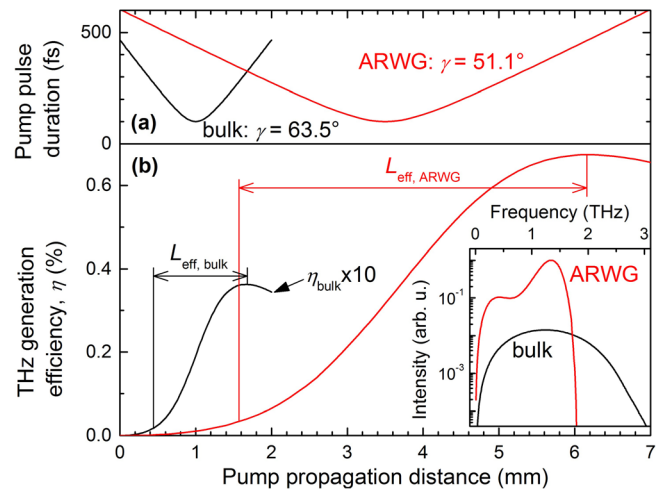


FIG. 4. Pump pulse duration (a) and the (cumulative) THz generation efficiency (b) vs. pump propagation distance for bulk and ARWG. The inset shows the THz spectra corresponding to the efficiency peaks.

angular and material dispersion in LN was taken into account. A frequency-dependent effective refractive index was considered, and an effective absorption coefficient in the THz range was defined as $\alpha_{\text{eff, THz}} = \alpha_{\text{THz}} \cdot P_{\text{core}}/P_{\text{total}}$, where α_{THz} is the absorption coefficient of bulk LN. Waveguide dispersion at the pump wavelength (1030 nm) was neglected for simplicity. This is justified by the practical limit of about 5 mm to the ARWG length, which is due to the small core thickness. For a 5 mm long ARWG with the worst case of 5 μm thickness and only 100 fs pulse duration, waveguide dispersion lengthens the pump pulse duration only by 6 fs. The ARWG length was approximately set to the effective interaction length for THz generation,^{13,19} or to the 5 mm maximum, to maximize the output THz energy. In each case, the LN core thickness was chosen to fit with the THz frequency of the spectral peak that of the bulk source, in order to facilitate a fair comparison. The core width was set to a minimum such that the peak pump intensity remained below 100 GW/cm^2 or the average below $\sim 40 \text{ kW}/\text{cm}^2$ (measured damage threshold at 300 kHz repetition rate²⁰), whichever was smaller.

The calculations predict an enhancement of the THz generation efficiency, $\eta_{\text{ARWG}}/\eta_{\text{bulk}}$, by more than a factor of 20 for 10 nJ pump pulse energy, as compared with bulk LN. At higher pump energies the enhancement factor is gradually

TABLE II. Design parameters and predicted performance of the ARWG THz source for various laser types.

Pump	Energy (μJ)	0.01	0.1	1	5
	Repetition rate (MHz)	100	10	1	1
	Pulse duration (fs)	100	200	300	300
	Average power (W)	1	1	1	5
	Average intensity (kW/cm^2)	40	40	30	30
	Peak intensity (GW/cm^2)	4	20	100	100
ARWG	LN core thickness (μm)	5	9	15	15
	Minimum LN core width (w) (mm)	1.8	1.0	0.8	4.1
	ARWG length (L) (mm)	5	5	5	5
THz	THz spectral peak (THz)	1.35	0.92	0.71	0.71
	THz energy (nJ)	6.6×10^{-2}	3.2	95	477
	THz average power (mW)	6.6	32	95	477
	Efficiency enhancement factor ($\eta_{\text{ARWG}}/\eta_{\text{bulk}}$)	22 \times	6.6 \times	2.5 \times	2.5 \times
	Spectral intensity enhancement factor	53 \times	18 \times	7.6 \times	7.6 \times

reduced. It is about 2.5 for μJ -level energies. Clearly, this reduction is due to the limited ARWG length, since the assumed 300 fs pulse duration would allow effective interaction lengths significantly longer than 5 mm. It is possible to accommodate even larger pump energies over the cross-section of the ARWG, but this may require to increase the core thickness, leading to larger $n_{\text{eff,THz}}$, smaller $P_{\text{core}}/P_{\text{total}}$, and lower THz generation efficiency. Here, a more in-depth analysis would require to consider wave guiding and possible multi-mode propagation of the pump, but this is out of the scope of the present discussion. We note that even in case of the largest predicted efficiencies ($\sim 10\%$), the simple model of OR used here can still be adequate, rather than a more complex one taking into account the influence of the THz field on the pump,²¹ as the THz field strength is significantly reduced by the penetration into the cladding.

A comparison of the peak THz spectral intensities of the ARWG and bulk cases reveals an enhancement of $53\times$ for 10 nJ pump and $7.6\times$ at the μJ -level (Table II), much larger than the efficiency enhancement. The reason for this is the larger dispersion of $n_{\text{eff,THz}}$ than that of the bulk refractive index of LN, which leads to a reduced THz spectral width for the ARWG, clearly visible in the inset of Fig. 4.

In summary, an absorption-reduced planar waveguide structure driven by TFPF was proposed for increasing the efficiency of THz pulse generation by OR of femtosecond laser pulses. Most of the THz power is propagating in the cladding with low THz absorption, thereby reducing losses. In case of LN core, it was shown that a smaller pulse front tilt angle is required for velocity matching than in bulk LN, thereby increasing the interaction length and hence the conversion efficiency. Practical considerations and expected performance were presented for the design of an ARWG THz source for a broad range of laser pulse energies and repetition rates.

The ARWG structure will expectedly enable highly efficient THz pulse generation in highly nonlinear materials having large absorption coefficient by using moderate pump energy delivered, for example, by compact fiber laser sources. The predicted more than one order of magnitude increase in the conversion efficiency opens up the possibility to build highly efficient and compact THz sources with

extremely high average output power. Such sources can find many applications in (nonlinear) THz spectroscopy, imaging, and security.

Financial support from Hungarian Scientific Research Fund (OTKA) Grant No. 113083 is acknowledged. J.A.F. acknowledges support from János Bolyai Research Scholarship (Hungarian Academy of Sciences). The present scientific contribution is dedicated to the 650th anniversary of the foundation of University of Pécs, Hungary.

- ¹S. B. Bodrov, A. N. Stepanov, M. I. Bakunov, B. V. Shishkin, I. E. Ilyakov, and R. A. Akhmedzhanov, *Opt. Express* **17**, 1871 (2009).
- ²M. I. Bakunov, B. Bodrov, and M. Hangyo, *J. Appl. Phys.* **104**, 093105 (2008).
- ³S. B. Bodrov, I. E. Ilyakov, B. V. Shishkin, and A. N. Stepanov, *Appl. Phys. Lett.* **100**, 201114 (2012).
- ⁴M. I. Bakunov, E. A. Mashkovich, M. V. Tsarev, and S. D. Gorelov, *Appl. Phys. Lett.* **101**, 151102 (2012).
- ⁵K. Suizu, K. Koketsu, T. Shibuya, T. Tsutsui, T. Akiba, and K. Kawase, *Opt. Express* **17**, 6676 (2009).
- ⁶W. Shi and Y. Ding, *Appl. Phys. Lett.* **82**, 4435 (2003).
- ⁷A. G. Stepanov, J. Hebling, and J. Kuhl, *Appl. Phys. B* **81**, 23 (2005).
- ⁸K. L. Vodopyanov and Y. Avetisyan, *Opt. Lett.* **33**, 2314 (2008).
- ⁹R. Zhichao, V. Georgios, K. L. Vodopyanov, M. M. Fejer, and S. Fan, *Opt. Express* **17**, 13502 (2009).
- ¹⁰J. Hebling, K. L. Yeh, M. C. Hoffmann, B. Bartal, and K. A. Nelson, *J. Opt. Soc. Am. B* **25**, 6 (2008).
- ¹¹L. Pálfalvi, J. Hebling, J. Kuhl, Á. Péter, and K. Polgár, *J. Appl. Phys.* **97**, 123505 (2005).
- ¹²J. Hebling, G. Almási, I. Kozma, and J. Kuhl, *Opt. Express* **10**, 1161 (2002).
- ¹³J. A. Fülöp, L. Pálfalvi, G. Almási, and J. Hebling, *Opt. Express* **18**, 12311 (2010).
- ¹⁴O. Gayer, Z. Sacks, E. Galun, and A. Arie, *Appl. Phys. B* **91**, 343 (2008).
- ¹⁵See http://www.tydexoptics.com/products/thz_optics/thz_materials/ for refractive indices and THz absorption coefficient of PMP.
- ¹⁶D. R. Grischkowsky, *Opt. Photonics News* **3**, 21 (1992).
- ¹⁷Y. S. Jin, G. J. Kim, and S. G. Jeon, *J. Korean Phys. Soc.* **49**, 513 (2006).
- ¹⁸B. E. A. Salech and M. C. Teich, *Fundamentals of Photonics* (John Wiley & Sons, Inc., 1991).
- ¹⁹J. A. Fülöp, L. Pálfalvi, M. C. Hoffmann, and J. Hebling, *Opt. Express* **19**, 15090 (2011).
- ²⁰W. Schneider, A. Ryabov, Cs. Lombosi, T. Metzger, Zs. Major, J. A. Fülöp, and P. Baum, *Opt. Lett.* **39**, 6604 (2014).
- ²¹K. Ravi, W. R. Huang, S. Carbajo, W. Wu, and F. Kärtner, *Opt. Express* **22**, 20239 (2014).